

Ridge National Laboratory).

Registry No. Dihexyl adipate, 110-33-8; neutron, 12586-31-1.

## References and Notes

- (1) Bernardo, J. J.; Burrell, H. In *Polymer Science*; Jenkins, A. D., E.; North-Holland: Amsterdam, 1972; Vol 1, p 537.
- (2) Ferry, J. D. *Viscoelastic Properties of Polymers*; Wiley: New York, 1980; p 486.
- (3) Nielsen, L. E. *Mechanical Properties of Polymers*; Reinhold: New York, 1962; p 168.
- (4) Theodorou, M.; Jasse, B. *J. Polym. Sci., Polym. Phys. Ed.* **1983**, *21*, 2263.
- (5) Schaefer, J.; Stejskal, E. O. *Top. Carbon-13 NMR Spectrosc.* **1979**, *3*, 384.
- (6) Eckman, R.; Alla, M.; Pines, A. *J. Magn. Reson.* **1980**, *41*, 440.
- (7) Doty, F. D.; Ellis, P. D. *Rev. Sci. Instrum.* **1981**, *52*, 1868.
- (8) Stejskal, E. O. U.S. Patent 4 446 430, May 1, 1984.
- (9) Stejskal, E. O.; Schaefer, J.; Steger, T. R. *Faraday Symp. Chem. Soc.* **1978**, *13*, 56.
- (10) Schaefer, J.; Sefcik, M. D.; Stejskal, E. O.; McKay, R. A. *Macromolecules* **1984**, *17*, 1118.
- (11) Schaefer, J.; McKay, R. A.; Stejskal, E. O.; Dixon, W. T. *J. Magn. Reson.* **1983**, *52*, 123.
- (12) Hester, R. K.; Ackerman, J. L.; Neff, B. L.; Waugh, J. S. *Phys. Rev. Lett.* **1976**, *36*, 1081.
- (13) Stoll, M. E.; Vega, A. J.; Vaughan, R. W. *J. Chem. Phys.* **1976**, *65*, 4093.
- (14) Waugh, J. S.; Huber, L. M.; Haeberlen, U. *Phys. Rev. Lett.* **1968**, *20*, 180.
- (15) Munowitz, M. G.; Griffin, R. G.; Bodenhausen, G.; Huang, T. H. *J. Am. Chem. Soc.* **1981**, *103*, 2529.
- (16) Munowitz, M. G.; Griffin, R. G. *J. Chem. Phys.* **1982**, *76*, 2848.
- (17) Mansfield, P.; Orchard, M. J.; Stalker, D. C.; Richards, K. H. *B. Phys. Rev.* **1973**, *37*, 90.
- (18) Rhim, W. K.; Elleman, D. D.; Vaughan, R. W. *J. Chem. Phys.* **1973**, *59*, 3740.
- (19) Burum, D. P.; Linder, M.; Ernst, R. R. *J. Magn. Reson.* **1981**, *44*, 173.
- (20) Spiess, H. W. *Colloid Polym. Sci.* **1983**, *261*, 193.
- (21) Herzfeld, J.; Berger, A. E. *J. Chem. Phys.* **1980**, *73*, 6021.
- (22) Schaefer, J.; Stejskal, E. O.; McKay, R. A.; Dixon, W. T. *Macromolecules* **1984**, *17*, 1479.
- (23) Wignall, G. D.; Child, H. R.; Samuels, R. J. *Polymer* **1982**, *23*, 957.
- (24) Hayashi, H.; Flory, P. J.; Wignall, G. D. *Macromolecules* **1983**, *16*, 1328.
- (25) Cooper, S. L.; Yarusso, D. J. *Macromolecules* **1983**, *16*, 1871.
- (26) Higgins, J. S.; Stein, R. S. *J. Applied Crystallogr.* **1978**, *11*, 346.
- (27) Maciel, G. E.; Kolodziejski, M. S.; Bertran, M. S.; Dale, B. E. *Macromolecules* **1982**, *15*, 686.
- (28) Haeberlen, U.; Waugh, J. S. *Phys. Rev.* **1968**, *175*, 453.
- (29) Pines, A.; Gibby, M. G.; Waugh, J. S. *J. Chem. Phys.* **1973**, *59*, 569.
- (30) Van Krevelen, D. W. *Properties of Polymers*; Elsevier: New York, 1976; p 395.
- (31) Edzes, H. T.; Veeman, W. S. *Polym. Bull. (Berlin)* **1981**, *5*, 255.
- (32) Skolnick, J.; Perchak, D.; Yaris, R.; Schaefer, J. *Macromolecules* **1984**, *17*, 2332.
- (33) Schaefer, J.; Stejskal, E. O.; Perchak, D.; Skolnick, J.; Yaris, R. *Macromolecules* **1985**, *18*, 368.
- (34) Volkenstein, M. V. *Configurational Statistics of Polymeric Chains*; Interscience: New York, 1963; pp 546-552.
- (35) Bueche, F. *Physical Properties of Polymers*; Interscience, New York, 1962; p 116.
- (36) Steger, T. R.; Schaefer, J.; Stejskal, E. O.; McKay, R. A. *Macromolecules* **1980**, *13*, 1127.

## Inverse Gas Chromatography. 4. The Diffusion Phenomena on the Column

Petr Munk,\* Timothy W. Card, Paul Hattam, Mohammad J. El-Hibri, and Zeki Y. Al-Saigh

Department of Chemistry and Center for Polymer Research, University of Texas at Austin, Austin, Texas 78712. Received August 22, 1986

**ABSTRACT:** Broadening of chromatographic peaks in inverse gas chromatography experiments was analyzed. An evaluation technique was designed, allowing calculation of gas-gas mutual diffusion coefficients of a number of probes at a number of temperatures, provided that this coefficient is known for a single probe at a single temperature from an independent experiment. Under a similar condition, mutual diffusion coefficients of various probes in amorphous polymers above the glass transition temperature may be measured at a number of temperatures. The method yielded a dependence of the diffusion volume of normal alkanes in the gas phase on the chain length. The diffusion constants of normal alkanes in polyisobutylene at a number of temperatures were also obtained.

## Introduction

Diffusion processes on gas chromatographic columns lead to broadening of the chromatographic peak. In traditional gas chromatography, the peak broadening is directly related to the resolving power of the columns and as such has received extensive theoretical interest.<sup>1,2</sup> There are two major factors that contribute to peak broadening: diffusion of the injected compound (probe) in the carrier gas and diffusion of the probe in the stationary phase. The former factor is characterized by the gas-phase mutual diffusion coefficient,  $D_g$ , and the latter factor is related to the liquid-phase mutual diffusion coefficient,  $D_L$ .

In the case of inverse gas chromatography (IGC) experiments, where a polymer is the stationary phase,  $D_L$  is a polymer-probe diffusion coefficient, an interesting quantity both experimentally and theoretically. Gray and Guillet<sup>3</sup> were able to measure the  $D_L$  coefficients of a small number of probes using as their stationary phase, low-density polyethylene coated onto glass beads. Miltz<sup>4</sup> in-

vestigated the diffusion of styrene in polystyrene at various temperatures using polystyrene coated onto Chromosorb P as the stationary phase.

During our recent IGC investigations we accumulated a large body of data using polyisobutylene (PIB) coated onto Chromosorb W as the stationary phase and linear alkanes from methane to undecane as probes. In the experiments, temperature, flow rate of carrier gas, and column loading were varied systematically. We have also designed a method of evaluating peak-broadening data from which both diffusion coefficients,  $D_g$  and  $D_L$ , may be obtained. The purpose of this paper is to determine the quality of the acquired data and the amount of information that may be extracted from them.

## Theory

We will follow the standard chromatographic approach in expressing the distribution of a probe on the column by means of the height equivalent to one theoretical plate

Table I  
Column Characteristics

column	length, cm	wt of support, g	wt of polymer, g	loading, wt %	$V_o$ , mL	$\gamma$
I	157.5	8.0040	0.0000	0.00	28.28	0.962
II	151.1	7.9760	0.2294	2.9	26.95	0.939
III	153.0	7.7980	0.5139	6.6	26.92	0.914
IV	154.3	7.8087	1.0084	12.9	25.68	0.947

(HETP),  $H$ . HETP is related to the number of theoretical plates  $N$  and to the physical length of the column  $L$  as  $H \equiv L/N$ .

The majority of theories are variations of the van Deemter theory,<sup>5</sup> which separates the factors influencing peak spreading into three groups: factors independent of flow rate, factors proportional to flow rate, and factors proportional to time. Since the length of time the probe spends on the column is inversely proportional to the flow rate,  $u$ , then the van Deemter equation may be expressed as

$$H = A + B/u + Cu = A + B/u + (C_g + C_L)u \quad (1)$$

The constant  $A$  describes the factors that are independent of flow rate; these factors are mainly related to differences in the time spent on the column by different portions (streamlines) of the carrier gas. On packed columns,  $A$  is called the eddy diffusion term and is related to the size of the support particles and the regularity of packing.

The constant  $B$  describes the time-dependent factors. Only the longitudinal diffusion of the probe, along the stream of the carrier gas, contributes significantly to  $B$ . Accordingly,  $B$  can be expressed as

$$B = 2\gamma D_g \quad (2)$$

where  $D_g$  is the coefficient of mutual diffusion of the probe and the carrier gas.  $\gamma$  is the tortuosity or structural factor and varies from column to column. Values of the structural factor have been reported<sup>1,2</sup> as lying between values of 0.5 and 0.7 for diatomaceous type supports.

The third term in eq 1 is related to peak spreading, which is due to slow transport of the probe within the column: the  $C_L$  term refers to the diffusion of the probe within the polymer, while the  $C_g$  term addresses the transport processes within the gas phase in the radial direction (i.e., perpendicular to the gas streamlines). According to van Deemter, the  $C_L$  term, related to diffusion in the liquid phase, reads

$$C_L = (8d^2/\pi^2)R_f(1 - R_f)/D_L \quad (3)$$

where  $d$  is the thickness of the (uniform) liquid phase and  $R_f$  is the well-known retardation factor. In a real column, the thickness,  $d$ , of the liquid phase is not uniform and thus  $d^2$  should be replaced by the average of the square of film thickness. This average is unfortunately not easily accessible experimentally, and it is therefore convenient to replace the expression in parentheses of eq 3 with another structural factor (thickness factor)  $\gamma_L$ . Equation 3 then reads

$$C_L = \gamma_L R_f(1 - R_f)/D_L \quad (4)$$

The van Deemter relations imply that diffusion results in peak broadening but that the peak remains Gaussian and also that the retention volume is not influenced by diffusion.

According to Gray and Guillet,<sup>6</sup> neither of these predictions is correct. As the  $C_L u$  term increases, the peak loses its Gaussian character and its maximum (taken as retention volume) shifts to lower values. Both phenomena are observed when the glass transition temperature is

approached, with an accompanying dramatic decrease of  $D_L$ . It is one of the goals of this study to find how good the van Deemter approximation is for rubberlike polymers coated on a porous support.

Theoretical expressions for  $C_g$  are numerous<sup>1,2</sup> but are complicated and difficult to use. We find it convenient to postulate  $C_g$  similarly to eq 4 as

$$C_g = \gamma_g R_f(1 - R_f)/D_g \quad (5)$$

$\gamma_g$  being another structural factor. We will see later that the exact form for this relation is not really important because the whole term will be found to be negligible within experimental errors.

Substituting eq 2, 4, and 5 into eq 1, we obtain

$$H = A + 2\gamma D_g/u + R_f(1 - R_f)(\gamma_L/D_L + \gamma_g/D_g)u \quad (6)$$

The above relationships for  $H$  were derived by assuming the flow rate of the gas along the column is constant. In real columns the gas velocity changes along the column as the carrier gas is expanding. This effect is accounted for by the introduction of two correction factors,<sup>1</sup>  $f$  and  $j$

$$f = [(P_i/P_o)^2 + 1]j^2/2 \quad (7)$$

$$j = [(P_i/P_o)^2 - 1]/[(P_i/P_o)^3 - 1] \quad (8)$$

Here,  $P_i$  and  $P_o$  denote the column inlet and outlet pressures, respectively. The expression for the average value of  $H$ ,  $\bar{H}$  applicable for the whole column, then reads

$$\bar{H} = f(A + 2\gamma D_g^0/u_0) + R_f(1 - R_f)u_0(j\gamma_L/D_L + f\gamma_g/D_g^0) \quad (9)$$

Here,  $u_0$  is the linear flow rate measured at the outlet of the column. In the case of unretained probes ( $R_f = 1$ ), as well as for extensively retained probes ( $R_f \rightarrow 0$ ), the last term in eq 9 vanishes without respect to the values of  $D_L$  and  $D_g^0$ . Thus, everything else being the same, the most peak broadening will be observed for probes with  $R_f = 0.5$ .

## Experimental Section

The experimental procedure was described in previous papers.<sup>7-9</sup> Columns were prepared from 1/4-in.-o.d. copper tubing packed with 60–80 mesh Chromosorb W (acid washed and treated with dimethyldichlorosilane) and coated by polyisobutylene. The intrinsic viscosity of the polyisobutylene in cyclohexane at 20 °C was 195 mL/g, corresponding to a viscosity-average molecular weight of 379 000. The characteristics of the columns are shown in Table I; helium was used as the carrier gas. The amount of probe injected onto the column was selected so as to remain safely below concentrations for which the concentration effect is significant,<sup>9</sup> as well as below injection quantities that lead to a nonlinear detector response.<sup>8</sup> Typical injection volumes were 10–50  $\mu$ L for gaseous probes and 0.01–0.1  $\mu$ L for liquid probes. The experiments were performed at three flow rates; approximately 8, 16, and 22 mL/min, volumes being measured at 25 °C.

In experiments designed to study peak broadening in the extra-column part of the chromatograph, the column was replaced by a short capillary. From these experiments the extra-column volume  $V_d$  was determined to be 1.96 mL. Injection volumes in these experiments had to be reduced tenfold to prevent saturation of the detector.

The permeability of propane in PIB was measured at three temperatures by direct permeation experiments using a film cast on mercury from a cyclohexane solution. The film was dried in

a vacuum oven for 5 days at 100 °C prior to its use. The permeation apparatus used for the measurements is of a stainless steel construction and has been described in detail elsewhere.<sup>10</sup> The steady-state permeability,  $P^*$ , and the diffusion time lag,  $\theta$ , can normally be both obtained from a single permeation experiment. However, due to the experimental difficulties associated with this particular polymer,  $\theta$  was not measured and  $D_L$  was calculated based on the  $P^*$  values together with solubilities  $k^*$ .

Due to its low  $T_g$ , the PIB film was tacky and difficult to handle at room temperature. As such, it was not possible to use it "as is" in the gas transport cell. To overcome this obstacle, the PIB film was first laminated onto a very thin film of low-density polyethylene (PE). This composite PIB/PE film was then studied in the permeation cell. The PIB permeability was determined by using the model of series permeation resistances. This model reads, for the present case

$$r_c = r_{\text{PIB}} + r_{\text{PE}} \quad (10)$$

For a given film, the permeation resistance (a direct experimental quantity) is related to  $P^*$  and the film thickness  $d$  by

$$r = d/P^* \quad (11)$$

Thus, measurement of the resistance of the composite,  $r_c$ , of the PE film resistance,  $r_{\text{PE}}$ , and of the PIB film thickness, readily yielded  $P^*$  for PIB. The resistance of the PE supporting film was found to account for only 2–3% of the resistance for the two-film composite. For further details on this treatment the paper by Chiou et al.<sup>11</sup> can be consulted.

### Data Analysis and Results

The direct experimental data comprise the retention time of the marker,  $t_m$ , the retention time of the probe,  $t_p$ , and the half-height time (the width of the peak at half its height in time units),  $t_{h/2}$ . These quantities are related to the retention volume of the probe,  $V_r$ , and to the half-height volume of the probe,  $V_{h/2}$ , as

$$V_r = V_0 t_p / t_m \quad (12)$$

$$V_{h/2} = V_0 t_{h/2} / t_m \quad (13)$$

Here  $V_0$  is the inside volume of the chromatograph equal to the retention volume of the marker. For each column we have evaluated  $V_0$  by routine calculations at a number of temperatures and flow rates. The values of  $V_0$  were constant within 1%.

For the study of diffusion phenomena on the column the average HETP,  $\bar{H}$ , and the linear flow rate at the column outlet,  $u_0$ , are required. These were calculated from

$$\bar{H} = (L/5.54)(V_{h/2}/V_r)^2 \quad (14)$$

$$u_0 = L/jt_m \quad (15)$$

where  $L$  is the column length and  $j$  is given by eq 8.

However, eq 14 and 15 need to be corrected to take into account the extra-column volume. The latter correction is based on the well-known behavior of Gaussian peaks; if a peak is subsequently broadened by several processes, then the square of the final peak width is the sum of the squares of all contributing processes. Accordingly, eq 14 and 15 should be written as

$$\bar{H} = (L/5.54)(V_{h/2}^2 - V_{h/2}^d)/(V_r - V_d)^2 \quad (16)$$

$$u_0 = LV_0/jt_m(V_0 - V_d) \quad (17)$$

Similarly,  $R_f$  should be calculated as

$$R_f = (V_0 - V_d)/(V_r - V_d) \quad (18)$$

Here,  $V_{h/2}^d$  is the half-height volume measured from the capillary experiments.

Gray and Guillet<sup>3</sup> based their calculations of the diffusion coefficient  $D_L$  on the plot of  $\bar{H}$  vs.  $u_0$ . According to

eq 1 and 3, the limiting slope at high values of  $u_0$  is proportional to  $1/D_L$  (provided that  $C_g$  is negligible compared to  $C_L$ ). We will show now that the dependence of  $\bar{H}$  on  $u_0$  may yield more information, specifically, the gas-phase diffusion coefficients  $D_g^0$ .

Let us first examine the diffusion behavior of probes that are not retained by the column, i.e., for which  $R_f = 1$ . For such probes the last term in eq 9 vanishes. Examples of such probes are the marker and relatively volatile probes studied on columns without polymer coating. Under these circumstances, eq 9 is conveniently rearranged as

$$\bar{H}u_0/f = 2\gamma D_g^0 + Au_0 \quad (19)$$

Thus a plot of  $\bar{H}u_0/f$  vs.  $u_0$  should yield  $2\gamma D_g^0$  as an intercept and  $A$  as the slope.

Before proceeding with the analysis, it is worthwhile to mention that peak broadening in the extra-column volume may also be described by eq 19. However, the nature of the gas flow within the plumbing is quite different from that inside the column and the parameters  $\gamma$  and  $A$  are likely to have quite different values. Moreover, the linear gas velocity  $u_0$  and the length  $L$  are poorly defined within the plumbing. Nevertheless, the effective value of  $u_0$  is proportional to  $1/t_m^d$  and  $\bar{H}$  is proportional to  $(t_p^d/t_{h/2}^d)^2$ , the superscript  $d$  referring to experiments performed with the capillary column. Consequently, eq 19 may be written in this case as

$$(t_p^d/t_{h/2}^d)^2/(t_m^d)^3 = a + b/t_m^d \quad (20)$$

where  $b$  is an instrumental constant and  $a$  is dependent on probe and temperature. We have plotted  $(t_p^d/t_{h/2}^d)^2/(t_m^d)^3$  vs.  $1/t_m^d$  for our probes and found that data could be correlated by eq 20, where the constant  $b$  was (within a large but acceptable experimental error) independent of temperature and probe. We have collected the values of  $a$ , smoothed them and together with a common  $b$  value used them in the calculation of  $(V_{h/2}^d)^2$  according to the relationship

$$(V_{h/2}^d)^2 = (V_d)^2(b + at_m V_d/V_0) \quad (21)$$

The largest value of  $a$  is for methane at 96.9 °C and was determined to be close to 1.5; the  $b$  value for all probes was found to be close to 0.6. For high-boiling probes at low temperatures, such as nonane at 38.4 °C, there is a slight retention by the plumbing even in the absence of the column. Under these circumstances, the  $a$  values were larger than expected. This is possibly accounted for by the fact that eq 19 is not a fair representation for systems in which retention is not negligible.

After correcting our data for the peak spreading inside the plumbing according to eq 16–18, we have evaluated the constant  $A$  for a number of probes at a number of temperatures using plots of  $\bar{H}u_0/f$  vs.  $u_0$  according to eq 19. An example of such a plot is shown in Figure 1. The best value applicable for all experiments within an acceptable experimental error was 0.03 cm. This value should be compared with the average diameter of the particles of the support. For 60–80 mesh support, the diameter is approximately 0.03–0.02 cm. Literature<sup>1,2</sup> would predict an  $A$  of about 0.4–0.3 cm for this support, a value some tenfold greater than our observed value.

Once the value of  $A$  has been established, then eq 9 may be rearranged as

$$(\bar{H} - A)u_0/f = 2\gamma D_g^0 + (\gamma_L/D_L + f\gamma_g/D_g^0)R_f(1 - R_f)u_0^2j/f \quad (22)$$

Table II presents a few values of  $(\bar{H} - A)u_0/f$  for methane to illustrate that the values for marker are independent

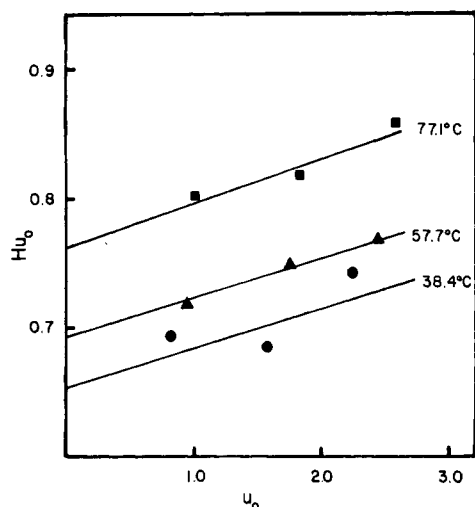


Figure 1. Dependence of  $\bar{H}u_0$  on  $u_0$  for butane (column I).

Table II  
Values of  $(\bar{H} - A)u_0/f$  for Marker on Column II

temp, °C	$(\bar{H} - A)u_0/f$ at approx flow rate		
	8 mL/min	16 mL/min	22 mL/min
38.4	1.31	1.38	1.31
57.7	1.51	1.52	1.44
77.1	1.51	1.60	1.51
96.9	1.81	1.69	1.71

of flow rate as expected ( $R_f = 1$ ).

In the next step, we needed to demonstrate that these values do represent the mutual diffusion coefficient  $D_g^0$ . We used for this purpose the reported dependence of  $D_g^0$  for the helium-methane system on temperature;<sup>12</sup>  $D_g^0$  should be proportional to the 1.75 power of absolute temperature  $T$ . Indeed, the values of  $\bar{H}u_0/T^{1.75}$  were independent of temperature as is apparent from Table III.

The next task was evaluation of the factor  $\gamma_g$ . For this purpose, we have utilized experiments for which we could safely neglect the diffusion of the probe through polymer, i.e., for which the parameter  $\gamma_L$  was zero. Such experiments involve uncoated columns (polymer thickness zero) under conditions where the probe is still retained by the inert support. Under these circumstances, the diffusion-mediated equilibration of the probes near the gas-support boundary operates as in any other IGC experiment, but no equilibration within the support is needed or possible. Thus, according to eq 22, a plot of  $(\bar{H} - A)u_0/f$  vs.  $R_f(1 - R_f)u_0^2j/f$  should yield a straight line with a slope of  $\gamma_g/D_g^0$ . Plots constructed in this manner, from uncoated column data, revealed that the slopes were negligible within the experimental error and thus we consider  $\gamma_g$  to be negligible.

Since we have determined that  $\gamma_g$  is negligible, plots of  $(\bar{H} - A)u_0/f$  vs.  $R_f(1 - R_f)u_0^2j/f$  for the coated columns should be linear and should yield  $2\gamma D_g^0$  as the intercept and  $\gamma_L/D_L$  as the slope. Examples of such plots are presented in Figures 2 and 3 illustrating the dependences on probe size and temperature.

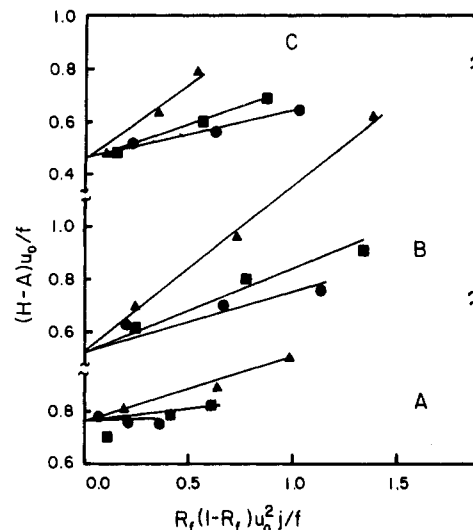


Figure 2. Plot of experimental data according to eq 22 illustrating the effect of probe size. Polyisobutylene at 77.1 °C. (A) Butane; (B) hexane; (C) octane. (●) Column II; (■) column III; (▲) column IV.

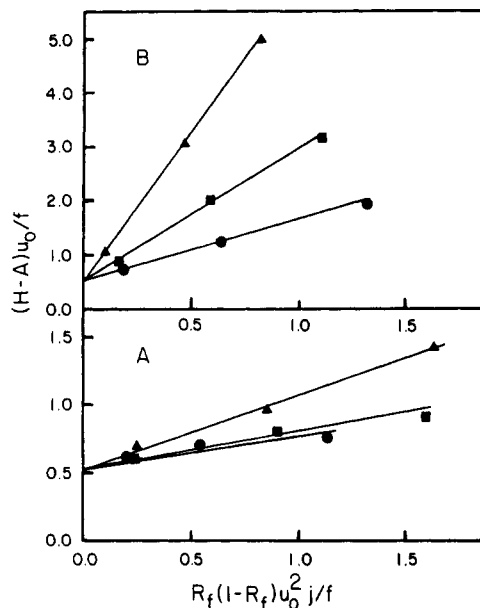


Figure 3. Plot of experimental data according to eq 22 illustrating the effect of temperature. (A) Hexane at 77.1 °C; (B) hexane at 38.4 °C. (●) Column II; (■) column III; (▲) column IV.

In order to analyze the intercepts we evaluated  $D_g^0$  for methane in helium using the method and data presented by Marrero and Mason.<sup>12</sup> We determined the value to be  $2.95 \times 10^{-5} T^{1.75}/P$ , where  $T$  is absolute temperature and  $P$  is a pressure factor, (atmospheric pressure/760 mmHg; for our system 0.984). Knowing the calculated value of  $D_g^0$  for methane and having the values of  $2\gamma D_g^0$  for our data on methane allowed us to determine the structural factor  $\gamma$  for each column. The average  $\gamma$  values are given in Table I.

Table III  
Values of  $(\bar{H} - A)u_0/f$  and  $(\bar{H} - A)u_0/fT^{1.75}$  for Methane

temp, °C	column I		column II		column III		column IV	
	x <sup>a</sup>	y <sup>b</sup>	x	y	x	y	x	y
38.4	1.331	5.76	1.333	5.78	1.306	5.66	1.354	5.87
57.7	1.393	5.43	1.488	5.80	1.436	5.59	1.456	5.67
77.1	1.553	5.48	1.542	5.44	1.443	5.08	1.558	5.49
96.9	1.836	5.88	1.740	5.57	1.733	5.55	1.769	5.66

<sup>a</sup>  $x = (\bar{H} - A)u_0/f$ . <sup>b</sup>  $y = (\bar{H} - A)u_0/fT^{1.75}$ .

Table IV  
Values of  $I/2\gamma T^{1.75}$  for Hexane

temp, °C	$I/2\gamma T^{1.75}$			
	column I	column II	column III	column IV
38.4	1.13	1.19	1.23	1.28
57.7	1.24	1.12	1.17	1.16
77.1	1.27	1.12	1.08	1.03
96.9	1.20	1.06	1.04	1.22

Table V  
Special Diffusion Volumes of *n*-Alkanes and Reduced Mutual Gaseous Diffusion Coefficients

<i>n</i>	<i>V</i>	av ( $PD_g^0/T^{1.75}$ ) × 10 <sup>5</sup>
1	26.1	2.95
2	46.7	2.11
3	71.1	1.69
4	95.8	1.44
5	120	1.27
6	142	1.14
7	192	0.99
8	241	0.87
9	305	0.76
10	374	0.68
11	451	0.61

After determining the structural factors,  $\gamma$ , for our four columns from our data on methane we could proceed with the analysis of our data for the other probes. From plots of  $(\bar{H} - A)u_0/f$  vs.  $R_f(1 - R_f)u_0^2j/f$  we obtained the intercept  $I = 2\gamma D_g^0$ . We have assumed, following the analysis of Fuller, Schettler, and Giddings,<sup>13</sup> that the gaseous diffusion constants for most probes are proportional to  $T^{1.75}$ . Thus we calculated the ratios  $I/2\gamma T^{1.75}$ , which were indeed found to be essentially constant, supporting the use of the 1.75 power temperature dependence. Examples of the reduced intercept are given in Table IV for hexane. In addition, we obtained the values of the reduced mutual gaseous diffusion coefficients,  $PD_g^0/T^{1.75}$ ; for our probes, the average values are presented in Table V. As an illustration of the reliability of the data a plot of average  $PD_g^0/T^{1.75}$  vs. the number of carbon atoms in the probe is presented in Figure 4.

Further, we utilized the Fuller, Schettler, and Giddings equation<sup>13</sup>

$$D_g^0 = \frac{1.00 \times 10^{-3} T^{1.75} (1/M_A + 1/M_B)^{1/2}}{P(V_A^{1/3} + V_B^{1/3})^2} \quad (23)$$

where  $M_A$  and  $M_B$  are molecular weights of the components—probe and helium for our system. The  $V_i$  values are the special diffusion volumes (quantities introduced by Fuller et al.<sup>13</sup>) for the molecules involved (2.88 for helium). According to Fuller et al.,<sup>13</sup> the special diffusion volumes of molecules are sums of the contributions of their constituent atoms.

We have evaluated the values of  $V$  (Table V) for our alkane probes and plotted them against the number of carbons in a logarithmic plot (Figure 5). For the smaller probes, the slope is almost exactly 1.0 as would be expected from the model of Fuller et al.<sup>13</sup> However, for probes longer than pentane, the special diffusion volume increases with a 1.9 power of the chain length. We believe that this relation contains information about the conformation of alkanes in the gas phase and we plan to return to this problem in future research.

What remains is to analyze the slopes of the plots of  $(\bar{H} - A)u_0/f$  vs.  $R_f(1 - R_f)u_0^2j/f$ , i.e., values of  $\gamma_L/D_L$ . It should be noted that these values contain dependencies on polymer loading and on temperature.  $\gamma_L$  is dependent on polymer loading (through the average thickness of the polymer layer) but independent of temperature. On the

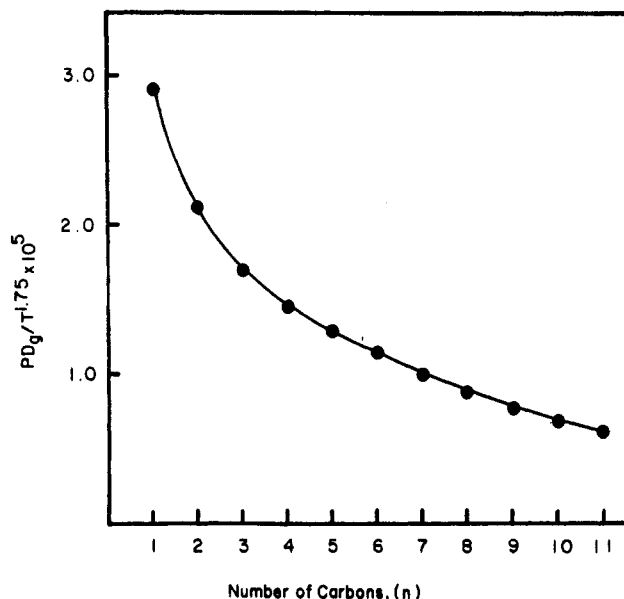


Figure 4. Dependence of the reduced mutual gaseous diffusion coefficients,  $PD_g^0/T^{1.75}$  for helium-*n*-alkanes on the number of carbon atoms *n*.

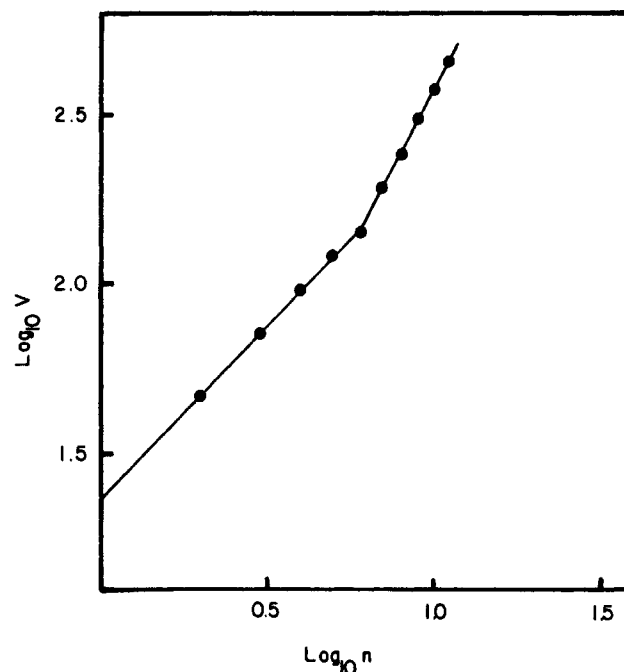


Figure 5. Logarithmic dependence of the special diffusion volume on the number of carbon atoms for *n*-alkanes.

other hand,  $D_L$  is dependent on temperature but independent of loading. The slopes obtained from our data are presented in Table VI; analysis of these slopes was performed as follows.

Plots of the logarithm of the slope vs. the number of carbon atoms were generated (Figure 6). In our opinion, all the plots possess the same shape irrespective of temperature and loading. Consequently we selected the shape of the curve with the least scatter of points (column IV at 38.4 °C, see Figure 6) and fitted the other dependencies by the same function multiplied by a factor  $s$ . The difference between the actual and reference curves on the logarithmic plots, such as those shown in Figure 6, is equal to logarithm of the factor  $s$ . A Zimm-type plot was then constructed for the logarithms of the factor  $s$  values as a function of inverse temperature and column loading (Figure 7). It is apparent that the factor  $s$  may be de-

Table VI  
Slopes of  $(\bar{H} - A)u_0/f$  vs.  $R_T(1 - R_T)u_0^2j/f$  Plots

temp, °C	column	no. carbon atoms							
		2	3	4	5	6	7	8	9
38.4	II	0.248	0.462	0.600	0.856	1.118	1.257	1.379	1.568
	III	0.315	0.635	1.343	2.044	2.805	3.172	3.062	3.260
	IV	0.296	1.566	2.941	4.028	5.488	6.138	6.385	
57.7	II				0.353	0.362	0.472	0.406	0.519
	III			0.328	0.482	0.835	0.743	0.785	0.957
	IV		0.474	0.879	1.115	1.374	1.658	1.633	1.993
77.1	II				0.038	0.124	0.137	0.115	0.085
	III				0.203	0.197	0.224	0.212	0.250
	IV			0.174	0.329	0.450	0.444	0.458	0.427
96.9	II				0.083	0.062	0.170	0.059	0.111
	III				0.079	0.070	0.075	0.060	0.110
	IV				0.196	0.138	0.150	0.120	0.175

Table VII  
Temperature Factors  $\tau(T)$  and Loading Factors  $\lambda(l)$

column IV		38.4 °C	
temp, °C	log $\tau(T)$	column	log $\lambda(l)$
38.4	0.000	IV	0.000
57.7	-0.590	III	-0.308
77.1	-1.108	II	-0.615
96.9	-1.638		

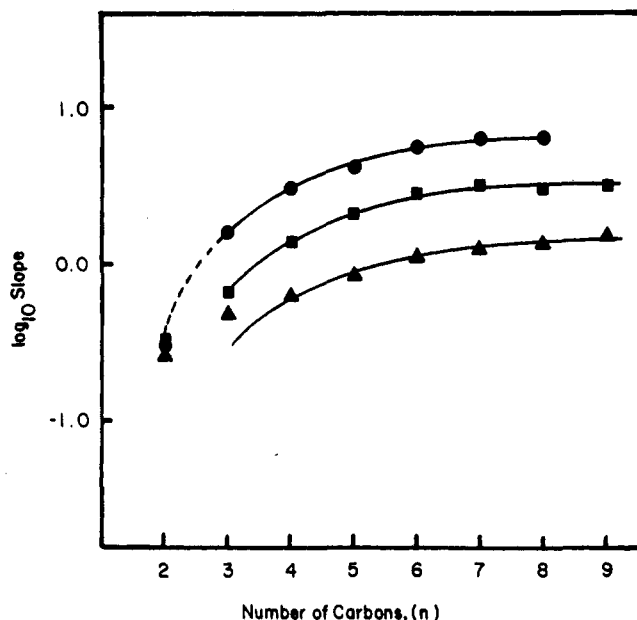


Figure 6. Dependence of the logarithm of the slope on the number of carbon atoms for  $n$ -alkanes at 38.4 °C: (▲) column II; (■) column III; (●) column IV.

composed into a temperature-dependent factor  $\tau(T)$  and a loading dependent factor  $\lambda(l)$ , where  $l$  is the loading of the column. The above calculations can be summarized as

$$S = S_{\text{ref}}(n)s = S_{\text{ref}}(n)\tau(T)\lambda(l) \quad (24)$$

where  $S$  is the slope and  $S_{\text{ref}}(n)$  is our reference slope determined from the plot of the logarithm of experimentally determined slopes vs. the number of carbon atoms,  $n$ , for our reference conditions: 38.4 °C and column IV. The factors  $\tau$  and  $\lambda$  are presented in Table VII and values of  $S_{\text{ref}}(n)$  are given in Table VIII. An example of experimental slopes and slopes calculated with the factors  $\tau$ ,  $\lambda$ , and  $S_{\text{ref}}(n)$  according to eq 24 is presented in Table IX for hexane.

The values of  $S$  calculated from eq 24 are equal to the ratios  $\gamma_L/D_L$ . Thus if we know  $D_L$  for any of our probes at any of our experimental temperatures, we can determine

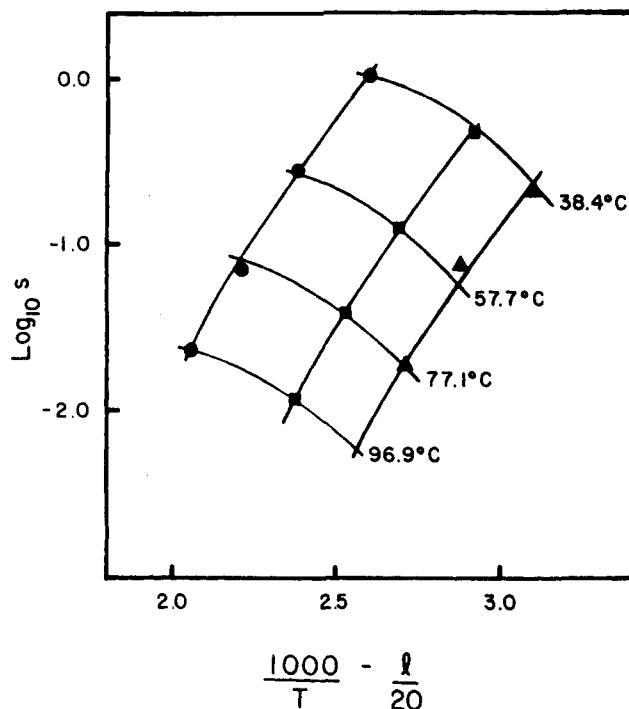


Figure 7. Zimm-type plot of the logarithm of the shift factor  $s$  on loading,  $l$ , and inverse temperatures as noted on the plot: (▲) column II; (■) column III; (●) column IV.

Table VIII  
Smoothed Values of the Reference Slope  $S_{\text{ref}}(n)$  (Column IV at 38.4 °C)

$n$	$S_{\text{ref}}(n)$	$n$	$S_{\text{ref}}(n)$
2	0.891	6	5.370
3	1.549	7	6.026
4	3.020	8	6.457
5	4.365	9	6.607

Table IX  
Comparison of Experimental Slopes and Calculated Slopes for Hexane

temp, °C	column	slope	
		exptl	calcd
38.4	II	1.12	1.30
	III	2.81	2.64
	IV	5.49	5.37
57.7	II	0.36	0.34
	III	0.84	0.68
	IV	1.37	1.38
77.1	II	0.12	0.10
	III	0.20	0.21
	IV	0.45	0.42
96.9	II	0.06	0.03
	III	0.07	0.06
	IV	0.14	0.12

**Table X**  
**Liquid Diffusion Coefficient of Propane in Polyisobutylene**

temp, °C	$D_L \times 10^8 \text{ cm}^2/\text{s}$	temp, °C	$D_L \times 10^8 \text{ cm}^2/\text{s}$
35.4	1.071	53.9	3.63
45.4	2.17		

the structural factor  $\gamma_L$  for our coated columns. Then we can evaluate the diffusion constants  $D_L$  of all probes at all experimental temperatures.

We have determined  $D_L$  for propane using a standard gas diffusion experiment across a polyisobutylene membrane as described in the Experimental Section. The values, obtained at three temperatures, are presented in Table X. The diffusion coefficients were calculated from the permeability data ( $P^*$ ) using the simple relation

$$D_L = P^*/k^* \quad (25)$$

where  $k^*$  is the solubility constant of the pressure-concentration ( $C_1$ ) relationship for the probe in the polymer

$$C_1 = k^*P_1 \quad (26)$$

The  $k^*$  values were obtained from the retention data gathered for propane on PIB. The following well-known expression was used:

$$k_H = RTv_p/M_1V_g \quad (27)$$

in which  $V_g$  is the specific retention volume,  $M_1$  is the molecular weight of the probe, and  $v_p$  is the specific volume of the polymer.  $k_H$ , Henry's law constant, is the inverse of  $k^*$  defined by eq 26.

The  $D_L$  values obtained with the above analysis are believed to be quite reliable. The  $D_L$  and activation energy for propane diffusion in PIB reported by Bixler et al.<sup>14</sup> are essentially identical with our results. The other source by Prager and Long<sup>15</sup> reports a  $D_L$  that is approximately half the value of Bixler and this work. The Prager data, however, appeared questionable because they were obtained from sorption kinetics studies rather than from more direct techniques.

Once  $D_L$  has been established, it is possible to evaluate the structural factors  $\gamma_L$ . Our most reliable data were at 38.4 °C on column IV and thus we used those data to obtain  $\gamma_L^{\text{IV}}$ . The structural factors for the other columns are simply related to that of  $\gamma_L^{\text{IV}}$  as

$$\gamma_L^{\text{III}} = \gamma_L^{\text{IV}}\lambda(l)^{\text{III}} \quad (28)$$

$$\gamma_L^{\text{II}} = \gamma_L^{\text{IV}}\lambda(l)^{\text{II}} \quad (29)$$

Factor  $\gamma(l)$  represents the ratio of structural factors for the column measured and the reference column. Since we have from eq 3 and 4 that

$$\gamma_L = 8\bar{d}^2/\pi^2 \quad (30)$$

where  $\bar{d}^2$  is the average square of the thickness of polymer on the support, then  $\lambda(l)$  should also be proportional to the average square of polymer thickness. If the layer of polymer were uniformly thick, then we would expect  $\lambda(l)$  to be proportional to the square of loading,  $l$ . If, on the other hand, the thickness were independent of loading and higher loadings were achieved by coating more of the support surface, then  $\lambda(l)$  should be independent of loading. The experimental situation is somewhere in the middle;  $\lambda(l)$  is more or less proportional to  $l$  (Figure 8).

Furthermore, once  $\gamma_L$  has been determined, it is possible to determine the average thickness,  $(\bar{d}^2)^{1/2}$ , of the polymer layer. For our type of support, the surface area is approximately  $1 \text{ m}^2/\text{g}$  and thus the predicted thickness of a homogeneous coating,  $d$ , can be calculated. Both  $(\bar{d}^2)^{1/2}$

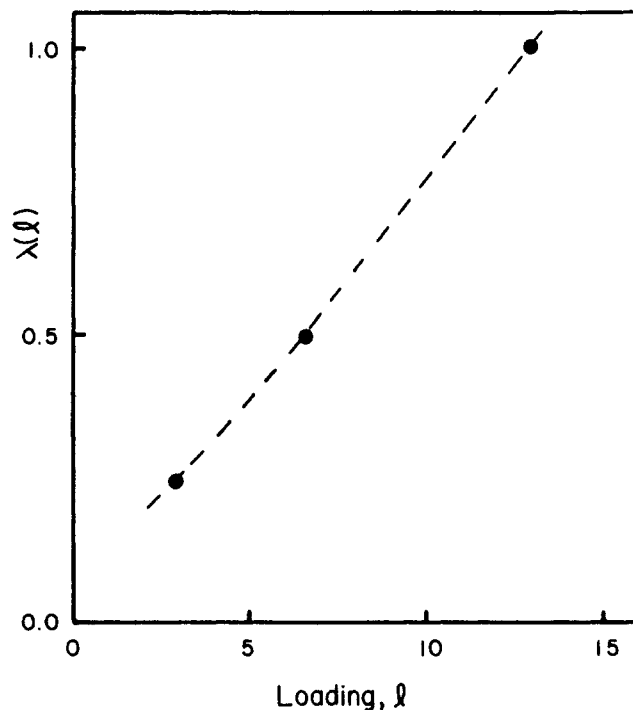


**Figure 8.** Dependence of structural factor ratios,  $\gamma(l)$ , upon loading,  $l$ .

**Table XI**  
**Structural Factors and Related Structural Parameters of the Columns**

column	$\gamma_L \times 10^9, \text{cm}^2$	$(\bar{d}^2)^{1/2} \times 10^6, \text{cm}$	$d \times 10^6, \text{cm}$
II	5.03	78.5	2.9
III	10.20	112.1	6.6
IV	20.73	160.0	12.9

**Table XII**  
**Relative Liquid Diffusion Coefficients of *n*-Alkanes in Polyisobutylene at Various Temperatures**

<i>n</i>	$D_L \times 10^8 (\text{cm}^2/\text{s})$ at			
	38.4 °C	57.7 °C	77.1 °C	96.9 °C
2	1.97	7.65	25.2	85.5
3	1.13	4.40	14.5	49.2
4	0.580	2.26	7.44	25.2
5	0.401	1.56	5.14	17.4
6	0.322	1.25	4.13	14.0
7	0.291	1.13	3.73	12.7
8	0.271	1.05	3.47	11.8
9	0.265	1.03	3.40	11.5

and  $d$  have been calculated and the homogeneous coating value,  $d$ , was found to be lower than  $(\bar{d}^2)^{1/2}$  by an order of magnitude. The values of  $\gamma_L$ ,  $(\bar{d}^2)^{1/2}$ , and  $d$  are presented in Table XI.

The factor  $\tau(T)$  represents the dependence of diffusion coefficient on temperature. This dependence is, according to our results, the same for all probes and would be interpreted from the temperature range employed as an Arrhenius dependence with activation energy of 14.2 kcal/mol (calculated from the slope of the  $\tau(T)$  dependence on temperature plot). The value obtained for the activation energy agrees reasonably well with the activation energy obtained for propane, from our direct measurements, which was 13.2 kcal/mol.

Since the diffusion coefficient for propane is known, it is possible to calculate the diffusion coefficients of all other probes at all experimental temperatures. Values of  $D_L$ , calculated from the smoothed slopes, for alkanes from ethane to nonane, are presented in Table XII.

## Conclusions

The inverse gas chromatography data for our experimental system, polyisobutylene-normal alkanes, were sufficiently precise and internally consistent to allow detailed analysis of the diffusion processes on the column.

A modified van Deemter's relation (eq 9) provided a satisfactory framework for the analysis. We were able to separate the four terms contributing to the height of an equivalent theoretical plate  $\bar{H}$ .

1. The flow-independent eddy diffusion term  $A$  was found to be 0.03 cm. This value is tenfold lower than quoted in the literature<sup>1</sup> for diatomaceous type supports.

2. The  $B$  term describing the longitudinal diffusion of the probe in the carrier gas conformed to behavior expected for a gas-gas mutual diffusion coefficient,  $D_g$ . It was possible to calculate relative values of  $D_g$  for all probes measured as well as their dependence on temperature. If any of these diffusion coefficients is known from independent sources, then absolute values of all  $D_g$ s may be calculated. In the present case,  $D_g$  for the helium-methane system was known. It allowed us to calculate the structural (or tortuosity) factor  $\gamma$ . This factor had close but not identical values for different columns. Its value was found to be about 0.9, i.e., somewhat larger than the value quoted in the literature<sup>1</sup> (0.5–0.7).

3. The  $C_g$  term and its related  $\gamma_g$  factor, describing the transversal diffusion of the probe in the gas phase, were negligibly small for the studied system (inert support, carrier gas, probes).

4. The fourth term,  $C_L$ , is the term most interesting for a polymer chemist. It provides access to the relative mutual diffusion coefficients,  $D_L$ , of polyisobutylene-normal alkanes and their temperature dependence. Again, using a single value measured in an independent experiment, we were able to calculate the absolute values of  $D_L$  as well as the thickness factor  $\gamma_L$ .

While the main goal of the present paper was to develop, test, and evaluate techniques of studying the diffusion processes on an inverse chromatography column, we have obtained other experimental data, which are interesting per se. One such finding is the dependence of the special diffusion volume on chain length for alkanes in the gas phase, which may provide clues to their conformation. Also, the diffusion coefficients of normal alkanes in polyisobutylene have been measured and their temperature dependence evaluated.

In summary, the analysis of the diffusion processes in inverse gas chromatography experiments may be valuable

in the following circumstances: (1) when gas-gas mutual diffusion coefficients of rather high boiling materials in gases, which can be used as carrier gases, are required; (2) when mutual diffusion coefficients of vapors in polymers are needed.

Both types of values are obtainable by other techniques only with large difficulties if at all. However, at the present time, the diffusion of probes in polymers is measurable by IGC techniques only over a limited temperature range. The lower limit is somewhat above the glass transition temperature: when the diffusion is too slow, the character of the dependences changes and the van Deemter equation is no longer applicable. The upper limit is governed by the magnitude of the  $C_L$  term. As  $D_L$  increases, the  $C_L$  term becomes too small and hence difficult to measure with confidence.

**Acknowledgment.** We are grateful to Hercules, Inc. (Educational Grant-in-Aid) and to National Science Foundation (Grant No. DMR-8414575) for support of this work.

**Registry No.** PIB, 9003-27-4; ethane, 74-84-0; propane, 74-98-6; butane, 106-97-8; pentane, 109-66-0; hexane, 110-54-3; heptane, 142-82-5; octane, 111-65-9; nonane, 111-84-2; decane, 124-18-5; undecane, 1120-21-4; methane, 74-82-8.

## References and Notes

- (1) Schupp, O. E. Chapter III, "Gas Chromatography" In *Technique of Organic Chemistry*; Perry, E. S., Weissberger, A., Eds.; Interscience: New York, 1968; Vol. XII.
- (2) Conder, J. R.; Young, C. L. *Physicochemical Measurement by Gas Chromatography*; Wiley: New York, 1979.
- (3) Gray, D. G.; Guillet, J. E. *Macromolecules* **1973**, *6*, 223.
- (4) Miltz, J. *Polymer* **1986**, *27*, 105.
- (5) van Deemter, J. J.; Zuiderweg, F. J.; Klinkenberg, A. *Chem. Eng. Sci.* **1956**, *5*, 271.
- (6) Gray, D. G.; Guillet, J. E. *Macromolecules* **1974**, *7*, 244.
- (7) Al-Saigh, Z. Y.; Munk, P. *Macromolecules* **1984**, *17*, 803.
- (8) Card, T. W.; Al-Saigh, Z. Y.; Munk, P. *Macromolecules* **1985**, *18*, 1030.
- (9) Munk, P.; Al-Saigh, Z. Y.; Card, T. W. *Macromolecules* **1985**, *18*, 2197.
- (10) Koros, W. J.; Paul, D. R.; Rocha, A. A. *J. Polym. Sci., Polym. Phys. Ed.* **1976**, *14*, 687.
- (11) Chiqui, J. S.; Barlow, J. W.; Paul, D. R. *J. Appl. Polym. Sci.* **1985**, *30*, 1173.
- (12) Marrero, T. R.; Mason, E. A. *J. Phys. Chem. Ref. Data* **1972**, *1*, 3.
- (13) Fuller, E. N.; Schettler, P. D.; Giddings, J. C. *Ind. Eng. Chem.* **1966**, *58*, 18.
- (14) Bixler, H. J.; Sweeting, O. J. In *The Science and Technology of Polymer Films*; Sweeting, O. J. Ed.; New York, 1968; Vol. 2, Chapter 1.
- (15) Prager, S.; Long, F. A. *J. Am. Chem. Soc.* **1951**, *73*, 4072.